Received: 8 April 2023 | Revised: 17 July 2023 | Accepted: 20 July 2023

DOI: 10.1002/elps.202300067

ELECTROPHORESIS

RESEARCH ARTICLE

Size separation of sodium dodecyl sulfate–proteins by capillary electrophoresis in dilute and ultra-dilute dextran solutions

Felicia Auer[1] | **Andras Guttman**[1,2]

[1]Translational Glycomics Group, Research Institute of Biomolecular and Chemical Engineering, University of Pannonia, Veszprem, Hungary

[2]Horváth Csaba Memorial Laboratory of Bioseparation Sciences, Research Center for Molecular Medicine, Doctoral School of Medicine, Faculty of Medicine, University of Debrecen, Debrecen, Hungary

Correspondence
Andras Guttman, Translational Glycomics Group, Research Institute of Biomolecular and Chemical Engineering, University of Pannonia, Veszprem, Hungary.
Email: guttmanandras@med.unideb.hu

Abstract

SDS capillary gel electrophoresis is a widely used in the biopharma and the biomedical fields for rapid size separation of proteins. However, very limited information is available on the use of dilute and ultra-dilute sieving matrices for SDS–protein analysis. Here, background electrolytes (BGEs) containing 1%–0% dextran were used in borate-based BGE to separate a protein sizing ladder (PSL) ≤225 kDa and the intact and subunit forms of a therapeutic monoclonal antibody (mAb). The separation performance for the PSL and mAb components differed significantly with decreasing dextran concentration. Ferguson and reptation plots were used to elucidate the separation mechanism. Highly diluted dextran solutions resulted in linear Ferguson plots for both solute types (*cf.* Ogston theory) in spite of this model assumes a rigid pore structure, thus cannot describe the separation mechanism in ultra-dilute polymer solutions with no reticulations. The saddle differences between the resolution of the PSL and the intact/subunit mAb forms in ultra-dilute dextran-borate matrices suggested the importance of shape selectivity, manifested by the adequate separation of the SDS covered intact as well as light and heavy chain subunits of the therapeutic mAb even at zero dextran concentration.

KEYWORDS

borate, capillary gel electrophoresis, dextran, SDS–proteins, ultra-dilute polymer

1 | INTRODUCTION

One of the most frequently used techniques for rapid protein analysis of up to the molecular mass range of several hundred kDa is sodium dodecyl sulfate (SDS) gel electrophoresis in slab [1] or capillary [2] (CGE) formats. Size separation of polyionic macromolecules such as SDS–proteins requires a sieving matrix including gels [3] or entangled polymer networks [4], since the negatively charged surfactant covered proteins assumable possess very similar surface charge densities, that is, not expected to separate in free solution [5]. Early attempts of CGE of SDS–protein complexes utilized cross-linked polyacrylamide gels [6], however, polymerizing the sieving

Abbreviations: HC, heavy chain; HEC, hydroxyethylcellulose; IPS, internal protein standard; LC, light chain; ngHC, nonglycosylated heavy chain; PSL, protein sizing ladder.

matrix inside the separation capillary frequently resulted in inhomogeneities and even bubbles. Albeit the use of non-cross-linked polymers above their entanglement threshold alleviated these issues [7], since the beginning of the new millennium transiently borate-cross-linked dextran matrices prevailed in CGE of proteins and became the industry standard, even in moderately diluted forms [8].

The most frequently used theories to describe the electromigration of polyionic macromolecules in gel electrophoresis are the Ogston [9], the extended Ogston [10] and the reptation [11] models. The Ogston model assumes a rigid gel structure with well-defined pore size distribution, in which case the unperturbed spherical solute molecules pass through the corresponding reticulations, resulting in size-based separation. The retardation coefficient in this case is defined by the Ferguson equation [12]:

$$ln\mu_{\text{eff}} = \mu_0 - K_{\text{R}}T \quad (1)$$

where μ_{eff} is the effective electrophoretic mobility (algebraic sum of the apparent mobility μ_{app} and the electroosmotic mobility μ_{EOF}), μ_0 is the free solution mobility, K_{R} is the retardation coefficient, and T is the gel concentration. The Ogston theory suggests linear Ferguson plots. The extended Ogston model allows the use of gel concentration–dependent retardation coefficients, that is, nonlinear Ferguson plots [10]. The concave Ferguson plots obtained with the use of commercial borate cross-linked dextran gels suggested rod-like shape of the electromigrating SDS–protein complexes [13]. Finally, the reptation theory describes the electromigration of large SDS–proteins passing through much smaller pore sizes via a head-first snake-like motion in high concentration gels, in which case the electrophoretic mobility and the molecular weight of the analyte is in an inverse relationship [14].

The possibility to separate polyionic macromolecules such as large DNA in ultra-dilute polymer solutions, well below the entanglement threshold, was suggested by Grossman and Soane [15]. Based on their theory, Barron and coworkers extensively studied the separation of nucleic acids in a wide size range of 72 to 23,000 bp using ultra-dilute hydroxyethyl cellulose (HEC) solutions. They reported that even at <0.15% polymer concentrations, dsDNA fragments of >2000 bp were still well separated via the separation mode of transient entanglement coupling, while the smaller dsDNA fragments of <600 were co-migrating [16]. According to their concept, large DNA molecules preferably entangled with the HEC chains and the smaller ones in a much lesser extent, that is, the large ones were well separated in ultra-dilute polymer solutions while the smaller ones were not.

In this work, we have evaluated the same approach to learn if SDS–proteins could also be separated in ultra-dilute polymer solutions and if so, by what separation mechanism. Special emphasis was given to the fact that both the borate-dextran adducts and the SDS–proteins are negatively charged, therefore, repelling each other, thus probably not supporting the transient entanglement coupling theory.

2 | MATERIALS AND METHODS

2.1 | Chemicals

Boric acid, Tris-base, EDTA.Na_2, glycerol, SDS, 2-mercapthoethanol, NaOH, and HCl were obtained from VWR. Dextran (2 MDa), iodoacetamid, and mesityl oxide were obtained from Sigma-Aldrich. The 10 kDa internal standard, the SDS-MW size standard, and the sample buffer (100 mM Tris-HCl, 1% SDS, pH 9) were purchased from Bio-Science Kft. The therapeutic mAb daratumumab (Darzalex) was from Janssen Biotech. The PNGaseF enzyme was from University of Pannonia (Veszprem, Hungary).

2.2 | Sample and gel-buffer preparation

Five microliters of SDS-MW Size Standard ladder (PSL: 20 to 225 kDa) was mixed with 2 μL of 10 kDa internal protein standard (IPS) and 5 μL of 2-mercaptoethanol (2-ME). Note that 5 μL of 20 mg/mL therapeutic mAb was denatured by the addition of 2 μL of denaturation mixture (Bio-Science Kft) followed by incubation at 70°C for 15 min. Then the *N*-glycans were partially released by the addition of 1 μL of PNGaseF (1.3 mg/mL) by applying 1-h incubation time at 37°C. For reduced mAb sample preparation, the endoglycosidase digested sample was mixed with 2 μL of 10 kDa IPS and 5 μL of 2-ME, followed by the addition of 80 μL SDS-MW sample buffer resulting in the light chain (LC), nonglycosylated heavy chain (ngHC), and heavy chain (HC) fragments. For nonreduced (intact) mAb sample preparation, 5 μL of therapeutic mAb was mixed with 2 μL of 10 kDa IPS, 5 μL of 250 mM iodoacetamide, and 80 μL of SDS-MW sample buffer. All samples were denatured at 70°C for 15 min.

The capillary electrophoresis running buffer consisted of 4.0% boric acid adjusted to pH 8.0 by Tris-base, followed by the addition of 2 mM EDTA, 10% (v/v) glycerol, and 0.2% SDS (final concentrations). Note that 200 mg dextran (2 MDa) was added to 20 mL buffer to obtain 1% polymer solution and stirred overnight at room temperature. This 1% dextran containing buffer was then diluted with the buffer system to obtain the 0.5%, 0.1%, 0.05%, and 0.01% final dextran concentration solutions.

TABLE 1 Important electrokinetic and physical parameters of the dilute and ultra-dilute dextran-based separation matrices.

Dextran concentration	1.00%	0.50%	0.10%	0.05%	0.01%	0.00%
EOF mobility $\times 10^{-9}$ (cm^2/V s)	4.08 ± 0.1	4.24 ± 0.1	4.29 ± 0.1	4.24 ± 0.1	4.17 ± 0.1	3.94 ± 0.1
Viscosity (mPa s)	7.3 ± 0.1	5.9 ± 0.1	5.1 ± 0.1	5.1 ± 0.1	5.0 ± 0.1	5.1 ± 0.1
Current (μA)	36.8 ± 0.2	37.3 ± 0.2	37.8 ± 0.2	37.9 ± 0.2	37.9 ± 0.2	37.9 ± 0.2

2.3 | Capillary SDS-gel electrophoresis

All experiments were performed on a P/ACE MDQ Capillary Electrophoresis System (Beckman Coulter) equipped with a UV detector (220 nm), utilizing a 20 cm effective length (30 cm total length, 50 μm id/ 375 μm od) bare fused-silica capillary. The capillary was conditioned prior to each measurement and between runs by rinsing for 3 min with 0.5 M NaOH, 1 min with 0.5 M HCl, 2 min with HPLC grade water, and 4 min with the actual separation gel-buffer system. The applied electric potential for the injection and separation steps were 5 and 15 kV, respectively, in reverse polarity mode (anode at the detection side). The intact mAb sample was electrokinetically injected by 5 kV for 20 s followed by the reduced mAb sample by 5 kV for 20 s (i.e., not mixed with the reducing agent containing sample). The 10 kDa IPS and the PSL were injected by 5 kV for 20 s. The separation temperature was 25°C. All measurements were made in triplicates ($n = 3$). For data acquisition and analysis, the 32Karat (version 8.0) software package (Beckman Coulter) and the Peakfit (version 4.12) software (SeaSolve) were used.

The effective mobilities were calculated as the algebraic sum of the apparent mobility and the electroosmotic flow (EOF) values. Since the batch-to-batch migration time reproducibility of the sieving matrices with ultradilute polymers was not perfect, the relative mobilities were calculated by dividing the effective mobility values by the effective mobility of the 10 kDa IPS and used for all calculations to obtain adequate comparability. The viscosities and EOF mobilities of all gel-buffer systems were measured by following the method previously published in [17].

3 | RESULTS AND DISCUSSION

In this paper, we report on the evaluation of dilute and ultra-dilute 2 MDa dextran solutions for the separation of the protein sizing ladder (20 to 225 kDa) as well as the intact and subunit forms of daratumumab, including the ngHC fragment. Dextran concentrations between zero and 1% were used with a constant 4% boric acid containing running buffer. Ferguson and reptation plots were utilized to evaluate the separation mechanism in ultra-dilute and zero polymer containing separation matrices also considering the shape selectivity term.

3.1 | Characterization of the separation media

First the separation matrices were characterized as the function of dextran concentration (1.00%, 0.50%, 0.10%, 0.05%, and 0%) with respect to viscosity, electroosmotic flow, and electric current (at 15 kV output potential), while all other BGE components were kept constant (425 mM Tris, 4% boric acid, 2 mM EDTA, and 10% glycerol). Table 1 shows that the highest EOF was obtained at 0.10% dextran concentration with decreasing values at lower and higher polymer contents. The viscosity and current values showed decreasing and increasing values with decreasing dextran concentrations, that is, oppositely affecting the EOF, probably resulting in the observed maximum.

3.2 | Analysis of the protein sizing ladder standards

Next, the PSL ranging from 20 to 225 kDa was analyzed in decreasing dextran concentration matrices (1.00%–0%), all containing 4% boric acid. Figure 1 compares the resulting electropherograms. At 1.00% and 0.50% dextran containing BGE, practically all seven peaks could still be recognized, although peaks 6 and 7 were greatly overlapping at 0.50% dextran concentration. Starting at 0.10% dextran content, only some of the lower MW standards could be identified (peaks 1–4, MW < 50 kDa, but peaks 1 and 2 overlapping), and the larger sample components (peaks 5–7, MW > 50 kDa) were co-migrating. This tendency was also observable at the lower (0.05% and 0.01%) and zero dextran concentrations, where in addition to the overlapping 10 kDa IPS and the 20 kDa PSL peaks, only the 35 kDa was distinguishable, the 50 kDa as a shoulder peak and the rest of the higher MW components were co-migrating. As a matter of fact, in this instance no size-based separation was expected without the presence of adequate concentration sieving matrix since these protein sizing molecules were constructed from non-PTM carrying polypeptides [18], that is, having no shape differences and assumable very similar surface charge densities in their SDS complex forms. However, based on our data showing the peak clusters of 1–2, 3, and 4–7, this assumption was not fully applicable to the partially separated lower MW components, probably due to slight intrinsic charge difference

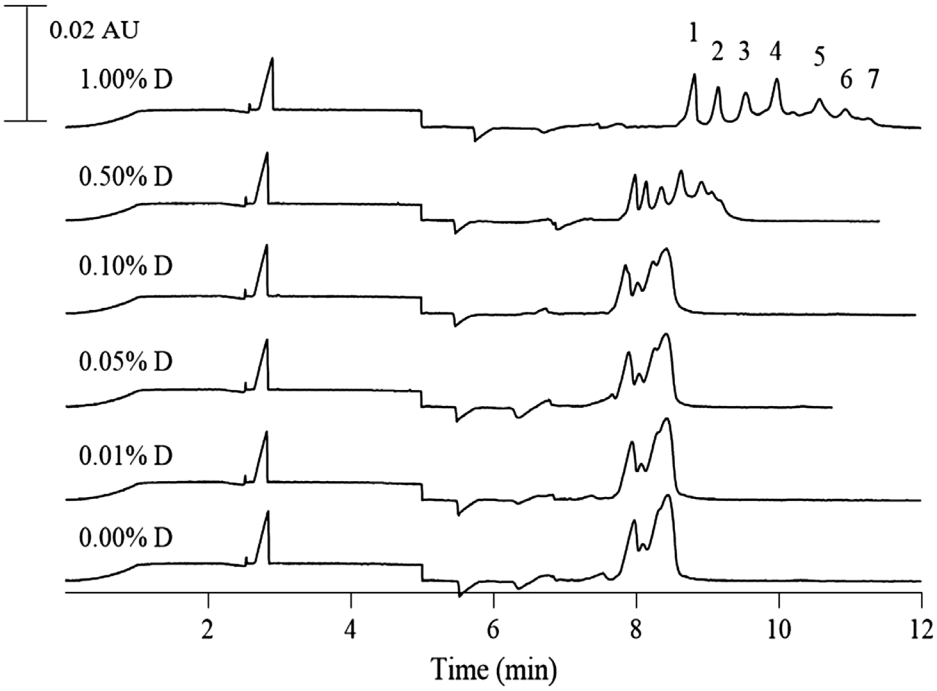

FIGURE 1 Capillary electrophoresis traces of the protein sizing ladder in decreasing dextran concentration separation matrices. Peaks: 1, 10 kDa internal standard; 2, 20 kDa; 3, 35 kDa; 4, 50 kDa; 5, 100 kDa; 6, 150 kDa; and 7, 225 kDa protein sizing standard. Conditions: bare fused silica capillary 20 cm effective length (30 cm total, 50 µm id); ultra violet (UV) detection at 220 nm; applied electric potential: 15 kV in reversed polarity mode (cathode at the injection side); separation temperature: 25°C; sample tray temperature: 20°C, electrokinetic injection: 5 kV for 20 s.

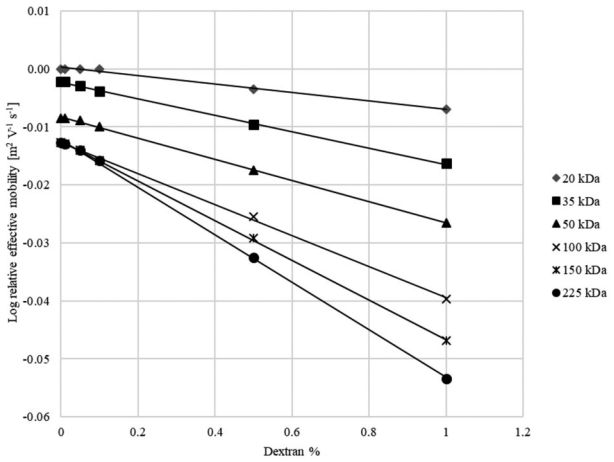

FIGURE 2 Ferguson plots of the separated protein sizing ladder components shown in Figure 1. The relative effective mobility values were calculated based on the electroosmotic flow (EOF) of the actual gel-buffer system and normalized for the mobility of the 10 kDa internal standard.

mediated changes in their charge to hydrodynamic volume ratios.

Figure 2 shows the Ferguson plots of the separated sample components in Figure 1. The linear lines were somewhat expected at ultralow dextran concentrations, based on our earlier results with the use of higher concentration gels [17]. The Ferguson plots of the large MW protein standards of 100 to 225 kDa were crossing each other at the zero gel concentration, which would be actually characteristic for pure MW-based size separation (Ogston model). However, in ultra-dilute polymer containing separation buffers with no reticulations, it was probably not the case. The lower MW standards, on the other hand, while their Ferguson plots were still converging to each other, not crossed at zero gel concentration, suggesting increasing free solution mobilities with decreasing molecule size, probably as the result of synergistic size-and charge-based separation [1]. The reptation plots of logarithmic relative effective mobility versus logarithmic reciprocal MW (Figure S1) with slopes of $\ll 1$, on the other hand, showed very similar behavior to large dsDNA fragments in ultra-dilute HEC solutions [16]; therefore, no reptation mechanism was considered.

3.3 | Analysis of the intact monoclonal antibody and its subunits including the nonglycosylated heavy chain fragment

The separation traces of the intact and subunit forms (LC, ngHC and HC) of the therapeutic mAb are shown in Figure 3, using the same separation matrices as in Figure 1.

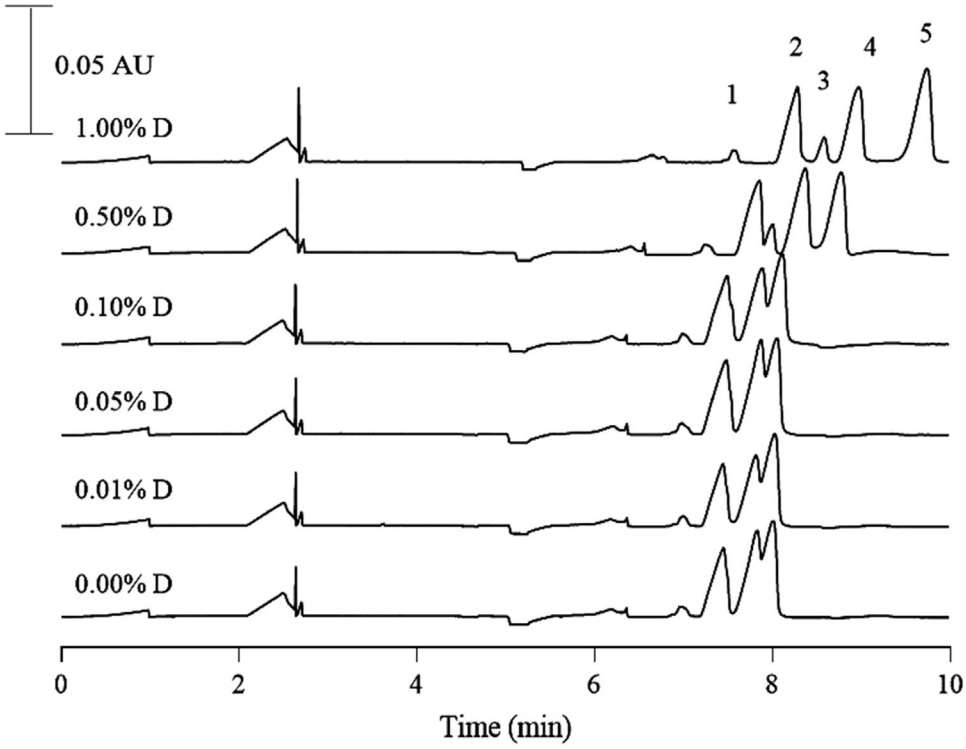

FIGURE 3 Capillary electrophoresis analysis of the intact and subunit forms of daratumumab in decreasing dextran concentration separation matrices. Peaks: 1, 10 kDa internal standard; 2, light chain (LC); 3, nonglycosylated heavy chain (ngHC); 4, heavy chain (HC); 5, intact monoclonal antibody (mAb). Conditions were the same as in Figure 1.

These electropherograms look quite different with the unexpectedly adequate separation of the 10 kDa IPS, and the LC, HC, and intact mAb, which were obtained even at zero dextran concentration background electrolyte. Please note that the ngHC peak gradually moved into the LC peak with decreasing dextran content and they started to co-migrate at <0.1% polymer concentrations.

The corresponding Ferguson are shown in Figure 4 revealing that the LC and ngHC fragments were crossing each other at zero gel concentration, i.e. their free solution mobilities were the same. The HC and intact mAb sample components, on the other hand, showed somewhat converging features, suggesting synergistic size and charge-based separation similar to that of the lower MW protein standards. The log relative effective mobility vs log reciprocal MW plots (Figure S2) featured significantly lower slope values than unity, so no reptation mechanism was contemplated for these sample components either.

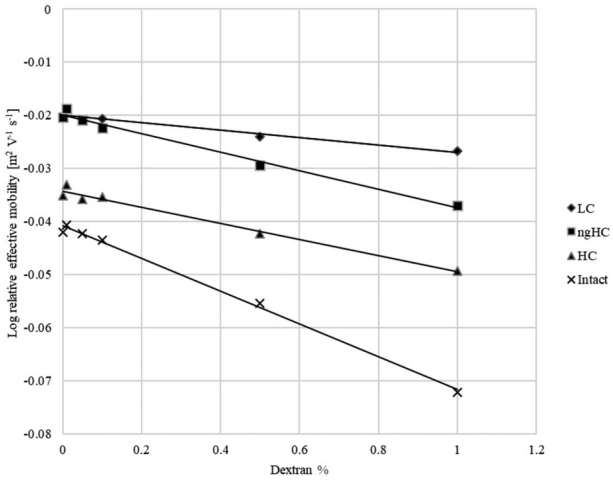

FIGURE 4 Ferguson plots of the separated sample components shown in Figure 3. The relative effective mobility values were calculated based on the electroosmotic flow (EOF) of the actual gel-buffer system and normalized for the mobility of the 10 kDa internal standard.

3.4 | Selectivity and resolution

The fact that some separation of the intact mAb and HC subunit from the LC fragment was still obtained at ultralow or even at zero dextran concentration suggested that earlier reported complexation phenomenon with 1:1 dextran-borate adducts [19] and configuration-based shape selectivity [17] must have played a role. Therefore, as a first approximation, we considered the apparent selectivity as the product of the following three components: (i) molecular weight based size selectivity (α_{MW}), (ii) borate-dextran

TABLE 2 Selectivity and resolution between the ngHC/ LC, HC/LC, HC/ngHC, and intact mAb/HC peak pairs.

Dextran concentration	1.00%	0.50%	0.10%	0.05%	0.01%	0.00%
α (ngHC/LC)	1.024 ± 0.002	1.012 ± 0.001	1.004 ± 0.001	Unity	Unity	Unity
Rs (ngHC/LC)	1.22 ± 0.01	0.62 ± 0.01	Zero	Zero	Zero	Zero
α (HC/LC)	1.083 ± 0.001	1.065 ± 0.001	1.053 ± 0.001	1.053 ± 0.001	1.050 ± 0.001	1.046 ± 0.001
Rs (HC/LC)	2.45 ± 0.02	1.73 ± 0.02	1.2 ± 0.01	1.11 ± 0.01	1.04 ± 0.01	1.01 ± 0.01
α (HC/ngHC)	1.029 ± 0.002	1.030 ± 0.002	1.031 ± 0.002	1.034 ± 0.002	1.035 ± 0.002	1.035 ± 0.002
Rs (HC/ngHC)	1.41 ± 0.02	1.27 ± 0.02	1.05 ± 0.01	1.04 ± 0.01	1.03 ± 0.01	1.00 ± 0.01
α (intact/HC)	1.054 ± 0.002	1.031 ± 0.002	1.019 ± 0.001	1.018 ± 0.001	1.017 ± 0.001	1.016 ± 0.001
Rs (intact/HC)	2.04 ± 0.02	1.10 ± 0.01	0.61 ± 0.01	0.56 ± 0.01	0.54 ± 0.01	0.51 ± 0.01

1:1 adduct mediated complexation selectivity with the glycosylated heavy chain (α_C), and (iii) shape selectivity (α_{shape}):

$$\alpha = \alpha_{MW} \times \alpha_C \times \alpha_{shape} \quad (2)$$

Equation (2) suggests that even without sieving ($\alpha_{MW} = 1$) and complexation ($\alpha_C = 1$) selectivities, the shape selectivity still can mediate some separation of the sample components. Table 2 lists the selectivity (α) and resolution (Rs) values between the ngHC/LC, HC/LC, HC/ngHC, and intact mAb/HC peak pairs. The Rs values decreased with decreasing dextran concentration for all sample component pairs. The selectivity values on the other hand decreased in case of the ngHC/LC, HC/LC, and intact/HC peak pairs, but increased between the ngHC and HC fragments. This latter observation was in close agreement with the suggestion of our earlier work [19], that is, better resolution can be obtained between glycosylated and nonglycosylated SDS–proteins at lower dextran concentrations in high borate environment, an important piece of information for separation optimization.

In view of the above, the last column in Table 2 (0% dextran) should represent the shape selectivity values (α_{shape}), since in that instance no dextran-borate adducts were present in the separation BGE to accommodate size- or complexation-based separation. The shape selectivity during the analysis of this particular intact mAb and its subunits probably originated from the bulky non-SDS-binding hydrophilic carbohydrate side chain on the HC fragment and the Y shape of the intact mAb. The resolution values for these solute pairs showed decreasing tendencies at lower dextran concentrations, but with a steeper decrease at the higher molecular weight range, as observable in the peak profiles of Figures 1 and 3. Since the ngHC (MW ~ 48 kDa) and the LC (MW ~ 24 kDa) did not possess any glycosylation PTM, their concomitantly negligible shape selectivities resulted in practically no separation at <0.1% dextran containing BGEs with very limited sieving capability.

3.5 | Migration mechanism

Comparative Ferguson plots between the similar molecular weight PSLs (20, 50, and 150 kDa, solid lines) and the subunits as well as the intact mAb molecules are shown in Figure 5 (24 kDa—LC, 48 kDa—ngHC, 49.5 kDa—HC and 145 kDa—intact, dotted lines). The respective Ferguson plots of 20, 50, and 150 kDa size standards and the LC, HC, and intact mAb were apparently parallel, that is, their free solution mobilities should be different, probably due to their shape differences as otherwise their charge state must be very similar considering the generally accepted 1.4 g SDS bound to 1.0 g protein rule of thumb. The ngHC plot, on the other hand, had a slope similar to the HC fragment but with higher mobility and crossing the LC plot at zero dextran concentration. Please note that the relative (to the 10 kDa IPS) effective mobility values of the PSL were greater than that of their corresponding size mAb-related counterparts (Table S1), suggesting greater hydrodynamic volumes for these latter ones with otherwise assumable similar surface charge densities, resulting in slower electromigration with countercurrent EOF.

Based on the results presented above, with diminishing sieving reticulations in the separation matrix, the Ogston (including the extended Ogston) and the reptation mechanisms could not describe the differential electromigration of SDS–proteins in ultra-dilute and no polymer containing BGE. The transient entanglement coupling mechanism suggested in [16] was not applicable either, due to the repelling characteristics of the negatively charged tetrahydroxyborate covered dextran chains and the SDS–protein complexes, as depicted in Scheme 1 by the horizontal double arrows.

Therefore, we suggest that at dextran concentrations of 1.0%–0.5%, the 1:1 adduct-based borate covered dextran chains with some possible 2:1 adducts (cross-link) may form some reticulations, resulting in adequate molecular sieving for the no PTM possessing MW sizing standards. At lower dextran concentrations, the negatively charged SDS–proteins could hit the randomly distributed negatively

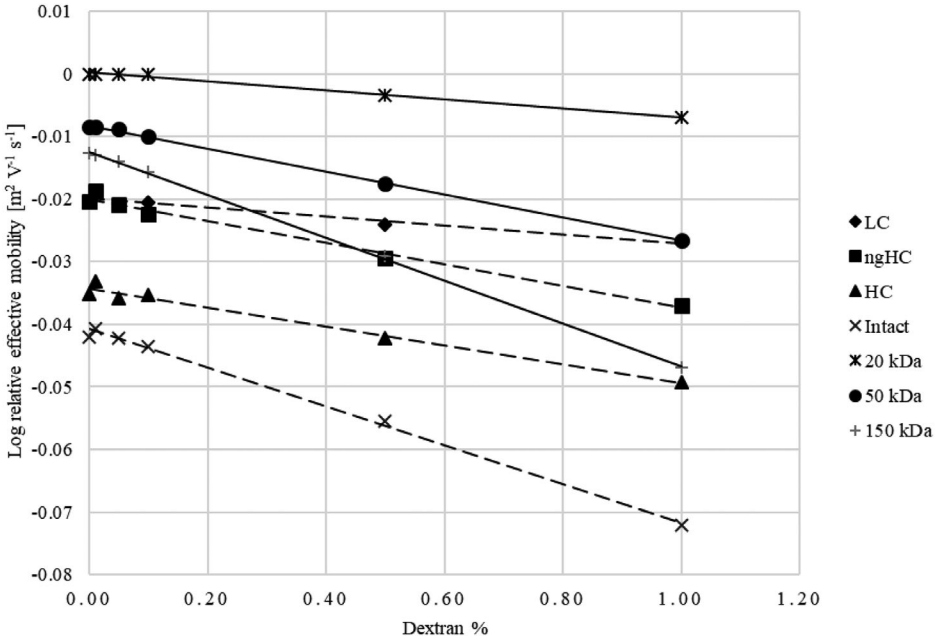

FIGURE 5 Comparative Ferguson plots of the 20, 50, and 150 kDa protein size standards (solid lines) as well as the light chain (LC), nonglycosylated heavy chain (ngHC), heavy chain (HC) fragments, and the intact monoclonal antibody (mAb) (dotted lines).

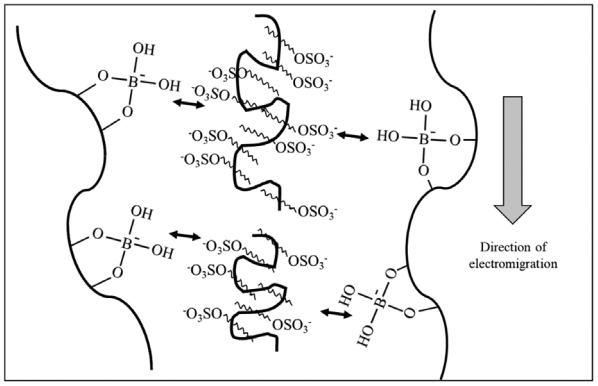

SCHEME 1 The repelling characteristics between the negatively charged tetrahydroxyborate covered dextran chains (1:1 adducts) and the sodium dodecyl sulfate (SDS)–protein complexes. The double arrows show the electrostatic repelling characteristics and the large vertical gray arrow shows the electromigration direction.

charged 1:1 borate dextran adduct chains in a non-sticking/non-entangled manner due to the charge repellence phenomenon, and swivel around until sliding off and migrate downstream as was suggested earlier by Calladine et al. [20]. This may actually happen with shorter rod-like proteins, while longer protein chains with multiple persistence length segments could hang like a thread and migrate further after sliding off, resulting in the observed separations at lower dextran concentrations, where the presence of cross-linking-based reticulations was highly unlikely.

4 | CONCLUDING REMARKS

In this work, dilute, ultra-dilute and zero (1%–0%, 2 MDa) dextran concentration BGEs were evaluated for the analysis of SDS–protein complexes by capillary electrophoresis. Please note that with this particular size dextran polymer, higher concentration matrices (up to 10%) have already been investigated [17] with optimized pH but we are planning to evaluate other MW dextran-based media in the future. The influence of temperature and dextran/borate concentration ratios were also addressed earlier [13, 17].

Separation of the PSL of 20 to 225 kDa and the intact and subunit forms (including the ngHC fragment) of daratumumab were used in the study. The corresponding Ferguson plots exhibited linear characteristics, similar to that of suggested by the Ogston theory, in spite of the fact that practically no reticulations were expected in these concentration range polymer solutions. The obvious resolution differences between the PSL and the mAb-related sample components pointed to the importance of shape selectivity, especially at zero dextran concentration BGEs. Based on the fact that neither the regular and extended Ogston nor the reptation model described the electromigration of these molecules at the ultralow polymer concentrations examined, the transient entanglement theory was also considered. However, as both of the borate-dextran chain adducts and the SDS–proteins were negatively charged, thus repelling each other, this was not an applicable option either.

Our suggested separation mechanism in dilute and ultra-dilute dextran-borate matrices is the intermittent nonsticky bumping of the SDS–proteins into the randomly distributed dextran chains resulting in pivoting for smaller and rope-like hanging for the larger proteins during their electromigration, consequently resulting in some size-based separation. In no polymer containing BGE, however, most probably the shape selectivity caused the observed separation of the otherwise assumable very similar surface charge density polyionic macromolecules. In case of lacking shape variances (e.g., glycosylation), even fragments with large MW differences but very similar surface charge densities were not separated as exemplified by the co-migration of the ngHC (~48 kDa) and LC (~25 kDa) subunits in dextran-free solutions. Nevertheless, during method optimization, one should certainly consider the favorable very fast separation times in dilute and ultra-dilute polymer solutions.

ACKNOWLEDGMENTS

The authors greatly appreciate the University of Debrecen TudFin grant #1G3DBK0CTUF247 support. This is contribution 205 of the Horváth Csaba Memorial Laboratory of Bioseparation Sciences.

CONFLICT OF INTEREST STATEMENT

The authors have declared no conflict of interest.

DATA AVAILABILITY STATEMENT

The data that support the findings of this study are available from the corresponding author upon reasonable request.

ORCID

Andras Guttman https://orcid.org/0000-0002-7838-082X

REFERENCES

1. Andrews AT. Electrophoresis theory, techniques, and biochemical and clinical applications. Oxford: Oxford Science Publications; 1986.
2. Guttman A, Hajba L. Capillary gel electrophoresis. Amsterdam: Elsevier; 2022.
3. Chrambach A, Rodbard D. Polyacrylamide gel electrophoresis. Science. 1971;172(3982):440–51.
4. Werner WE, Demorest DM, Stevens J, Wiktorowicz JE. Size-dependent separation of proteins denatured in SDS by capillary electrophoresis using a replaceable sieving matrix. Anal Biochem. 1993;212(1):253–8.
5. Righetti PG, Stoyanov AV, Zhukov MY. The proteome revisited: Theory and practice of all relevant electrophoretic steps. Part II. Methodology, Amsterdam: Elsevier; 2001. p. 217–74.
6. Cohen AS, Karger BL. High-performance sodium dodecyl sulfate polyacrylamide gel capillary electrophoresis of peptides and proteins. J Chromatogr. 1987;397:409–17.
7. Hunt G, Nashabeh W. Capillary electrophoresis sodium dodecyl sulfate nongel sieving analysis of a therapeutic recombinant monoclonal antibody: a biotechnology perspective. Anal Chem. 1999;71(13):2390–7.
8. Sänger-van de Griend CE. CE-SDS method development, validation, and best practice—an overview. Electrophoresis. 2019;40(18–19):2361–74.
9. Ogston AG. The spaces in a uniform random suspension of fibres. Trans Faraday Soc. 1958;54:1754–7.
10. Tietz D, Chrambach A. Computer simulation of the variable agarose fiber dimensions on the basis of mobility data derived from gel electrophoresis and using the Ogston theory. Anal Biochem. 1987;161(2):395–411.
11. Lumpkin OJ, Déjardin P, Zimm BH. Theory of gel electrophoresis of DNA. Biopolymers. 1985;24(8):1573–93.
12. Ferguson KA. Starch-gel electrophoresis—application to the classification of pituitary proteins and polypeptides. Metabolism. 1964, 13(Suppl):985–1002.
13. Filep C, Guttman A. The effect of temperature in sodium dodecyl sulfate capillary gel electrophoresis of protein therapeutics. Anal Chem. 2020;92(5):4023–8.
14. Guo XH, Chen SH. Reptation mechanism in protein-sodium-dodecylsulfate (SDS) polyacrylamide-gel electrophoresis. Phys Rev Lett. 1990;64(21):2579–82.
15. Grossman PD, Soane DS. Capillary electrophoresis of DNA in entangled polymer solutions. J Chromatogr. 1991;559(1–2):257–66.
16. Barron AE, Blanch HW, Soane DS. A transient entanglement coupling mechanism for DNA separation by capillary electrophoresis in ultradilute polymer solutions. Electrophoresis. 1994;15(5):597–615.
17. Guttman A, Filep C, Karger BL. Fundamentals of capillary electrophoretic migration and separation of SDS proteins in borate cross-linked dextran gels. Anal Chem. 2021;93(26):9267–76.
18. Millipore E. Protein Markers 10-225 kDa;BIO-69079, 2019.
19. Filep C, Guttman A. Effect of the monomer cross-linker ratio on the separation selectivity of monoclonal antibody subunits in sodium dodecyl sulfate capillary gel electrophoresis. Anal Chem. 2021;93(7):3535–41.
20. Calladine CR, Collis CM, Drew HR, Mott MR. A study of electrophoretic mobility of DNA in agarose and polyacrylamide gels. J Mol Biol. 1991;221(3):981–1005.

SUPPORTING INFORMATION

Additional supporting information can be found online in the Supporting Information section at the end of this article.

How to cite this article: Auer F, Guttman A. Size separation of sodium dodecyl sulfate–proteins by capillary electrophoresis in dilute and ultra-dilute dextran solutions. Electrophoresis. 2023;1–8. https://doi.org/10.1002/elps.202300067